



HAL
open science

Instabilities during dispersion flow through porous media : pore-size effect

Malgorzata Niespodzinska, Jean-Paul Gaudet, Pascale Royer, Jean-Louis Auriault

► **To cite this version:**

Malgorzata Niespodzinska, Jean-Paul Gaudet, Pascale Royer, Jean-Louis Auriault. Instabilities during dispersion flow through porous media : pore-size effect. 2nd Biot conference on poromechanics, Aug 2002, Grenoble, France. pp.515-519. hal-01718790v1

HAL Id: hal-01718790

<https://hal.science/hal-01718790v1>

Submitted on 1 Aug 2018 (v1), last revised 31 May 2022 (v2)

HAL is a multi-disciplinary open access archive for the deposit and dissemination of scientific research documents, whether they are published or not. The documents may come from teaching and research institutions in France or abroad, or from public or private research centers.

L'archive ouverte pluridisciplinaire **HAL**, est destinée au dépôt et à la diffusion de documents scientifiques de niveau recherche, publiés ou non, émanant des établissements d'enseignement et de recherche français ou étrangers, des laboratoires publics ou privés.

Instabilities during dispersion flow through porous media: pore-size effect

M. Niespodzinska

Geotechnical Dept., Faculty of Civil and Environmental Engineering, Technical University of Gdańsk and Laboratory Soils, Solids and Structures UMR CNRS 5521, CNRS, UJF, INPG

J.-P. Gaudet

Laboratory Transfer Studies in Hydrology and Environment UMR 5564, CNRS, INPG, IRD, UJF

P. Royer & J.-L. Auriault

Laboratory Soils, Solids and Structures UMR CNRS 5521, CNRS, UJF, INPG

ABSTRACT: We investigate experimentally and theoretically the instabilities which can occur during the vertical isothermal movement of two miscible fluids through a column of porous medium in the regime of mechanical dispersion. For the experiments we consider a non-deformable, homogenous and isotropic medium. There is no chemical or biological reaction during the experiments. Flow instabilities that occur during the tests depend upon numerous factors such as: solute density, viscosity, dispersion, flow velocity and pore diameter. We analyze the experimental results and we discuss the mechanisms of these instabilities.

1 INTRODUCTION

Instabilities in dispersion flow, known as a fingering effect, occur in many different engineering fields or technological processes which involve fluid flow through porous media (oil recovery, pollution and remediation of soils, groundwater flow, saline water intrusions, geothermal wells, filtration). It was first studied by Hill (1952) who carried out experiments on flow of sugar liquors due to water in columns of granular media. He explained the appearance of instabilities by the pressure difference due to small perturbations over the interface between the miscible fluids. Perrine (1961) and Heller (1966) studied the effect of diffusion on this phenomenon. Dumore (1964) and Schowalter (1965) found out that both the density and the viscosity contrasts with respect to the concentration played an important role in fluid flow stability. Wooding (1959) established the first stability criterion for two miscible fluids. Later, new techniques were developed to describe this phenomenon and it was studied more precisely taking into account different aspects like: influence of temperature or dispersion anisotropy (Quintard, 1979, 1980, 1983, Routaboul, 1980, 1981). More recently, numerical simulations were performed (Tan et al., 1986, Homsy, 1987, Zimmerman et al., 1991, Manickam et al., 1995).

This work is aimed towards investigating experimentally and theoretically the occurrence of

instabilities during vertical flow of two miscible fluids through a column packed with glass beads.

Our goal is to determine the pore size influence, which is related to the bead size. Then, we analyze experimental results and observations on the basis of the criterion proposed by Wooding (1959) and for the critical values calculated by Bues (1987) by means of a perturbation method.

The fingering effect which occurs in the porous medium during unstable fluid flow is a function of different parameters such as: solute density ρ , viscosity μ , flow velocity v and diameter of pores d . For simplicity, a vertical isothermal movement of two miscible incompressible fluids at constant velocity in a column packed with beads is considered. Stable and unstable flows during a vertical ascending and descending movement were investigated. The porous medium is assumed to be non-deformable, homogenous and isotropic, and no chemical or biological reaction occurred.

2 EXPERIMENTS

2.1 Experimental set-up

The experimental set-up (Fig.1) consisted of a chromatographic column filled up with glass beads, a peristaltic pump (to ensure constant fluid flow through

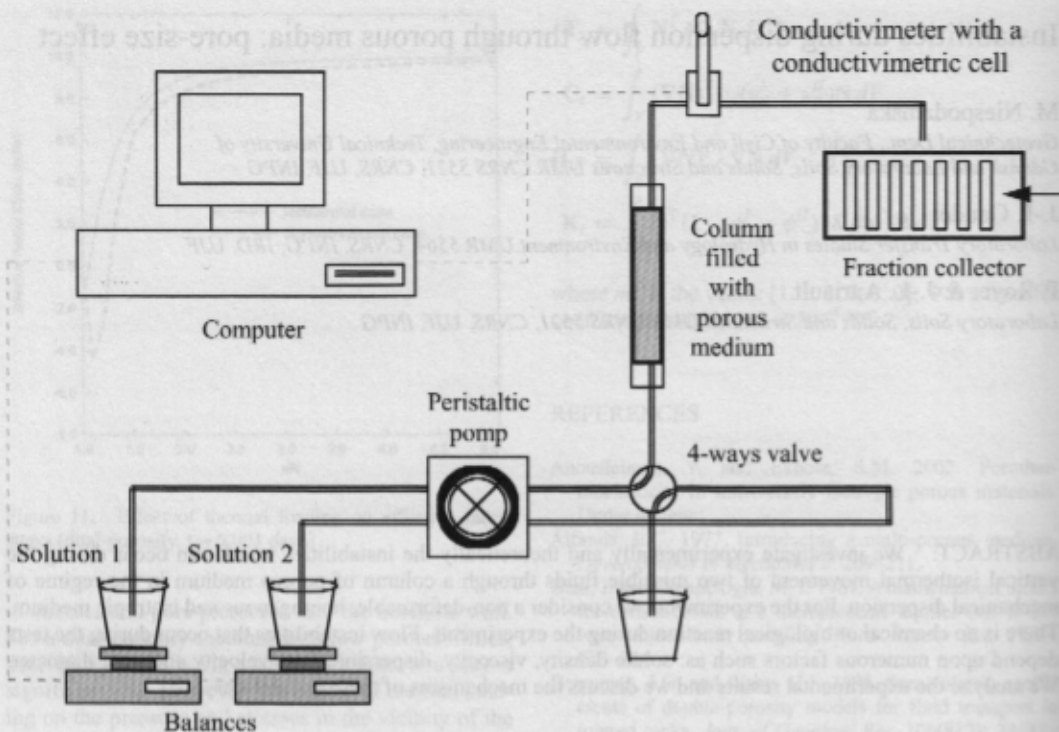


Figure 1. Experimental set-up.

the column), a conductivity-meter with a conductivimetric cell (to control concentration changes with respect to time) and a fraction collector to gather solute samples for further chemical analyses. Two distinct glass bead diameters ($d_1 = 1$ mm and $d_2 = 4$ mm) were successively considered.

2.2 Physical characteristics

The experiments were performed in a column with a length of $L = 31.6$ cm and with a diameter of $d_c = 2.6$ cm. For the first type of beads with diameter of $d_1 = 1$ mm the characteristic parameters were the following: the bulk density $\rho_{d1} = 1.53$ g/cm³, the porosity $n_1 = 0.423$ and the volumetric water contents $\theta_{s1} = 0.384$. For the second type of beads with a diameter $d_2 = 4$ mm the characteristic parameters were: bulk density $\rho_{d2} = 1.50$ g/cm³, porosity $n_2 = 0.434$ and volumetric water contents $\theta_{s2} = 0.422$. In both cases fluid flow through the column was permanent since the porous medium was homogenous and isotropic, and the volumetric water discharge was kept constant ($Q = 68.4$ cm³/h), by means of the peristaltic pump. Darcy's velocity was $q = 12.9$ cm/h. For this velocity, two slightly different pore velocities were obtained with beads d_1 and d_2 : $v_1 = 30.5 \times 10^{-3}$ cm/s

and $v_2 = 33.5 \times 10^{-3}$ cm/s. These experiments were also performed in a column with a length of $L = 46$ cm and a diameter of $d = 6$ cm and similar results were obtained which proves that there was no boundary effect. To make the effect of instabilities more visible, the experiments with beads of size d_2 were also performed using a color tracer and under the same hydrodynamic conditions. In this case, the injected solute B with a larger concentration was tinted with rhodamine (the first solute A remained transparent).

2.3 Experimental procedure

The permanent fluid flow regime was established in the column at the natural saturation of $\theta = \theta_s$. For the experiments we used KCl at two different concentrations: $C_A = 0.1$ g/l and $C_B = 1.0$ g/l. Firstly, solute A (KCl at 0.1 g/l) was injected in the column at constant rate. As soon as the permanent fluid flow regime was reached, a rectangular impulse of $0.85 V_0$ of solute B (KCl at 1.0 g/l) was injected into the column. The pore volume V_0 denotes the total volume of water within the column; thus, under total saturation conditions, V_0 is equal to the total volume of pores. The evolution of the concentration with respect to time is measured at the column exit by means of the conductivity-meter.

Simultaneously, solute samples were collected by the fraction collector at equal time. The weight of the saturated column was measured before each experiment and checked afterwards, in order to verify that the water content volume remains unchanged.

2.4 Results

The breakthrough curves (BTC) that describe the evolution of concentration with respect to time are deduced from the conductivity values which have been measured during the experiments and also from the chemical analyses which have been afterwards performed on the collected solute samples (Pallud, 2000). Let define the relative concentration C/C_0 by:

$$\frac{C}{C_0} = \frac{C - C_A}{C_B - C_A} \quad (1)$$

The normalized BTC-curves that describe the evolution of the relative concentration C/C_0 with respect to the relative volume V/V_0 are plotted on Figure 2.

The analysis of these breakthrough curves is performed by applying the moment method (Jury et al., 1990; Schoen et al., 1999): for each curve the successive temporal moments of order 0 and 1 are numerically calculated in order to determine the mass balance MB , the average residence time t_r of the solute in the column and the retardation factor R (Jury et al., 1990). The dispersion coefficient D can be determined by comparing the experimental breakthrough curves with the theoretical breakthrough curves (see Fig. 2). These latter are obtained by solving the convection dispersion model (CD).

$$\frac{\partial C}{\partial t} = D \frac{\partial^2 C}{\partial x^2} - v \frac{\partial C}{\partial x} \quad (2)$$

Figure 2 shows three different experimental results corresponding to different flow directions and bead sizes.

- a) stable (ascending or descending) flow; bead size: 1 mm
- b) unstable ascending flow; bead size: 4 mm
- c) unstable descending flow; bead size: 4 mm.

Comparison of the results calculated from the CD model (solid line) with the experimental breakthrough curves (points) shows the influence of pore size.

In case a, the curve 2a is obtained whatever the flow direction. Therefore, the flow is stable. It can be seen from curve 2a that the experimental results are in good agreement with the theoretical results obtained by solving Eq. 2. The mass balance is equal to $MB_1 = 0.98$ ($MB = 1$ means that the total injected mass was

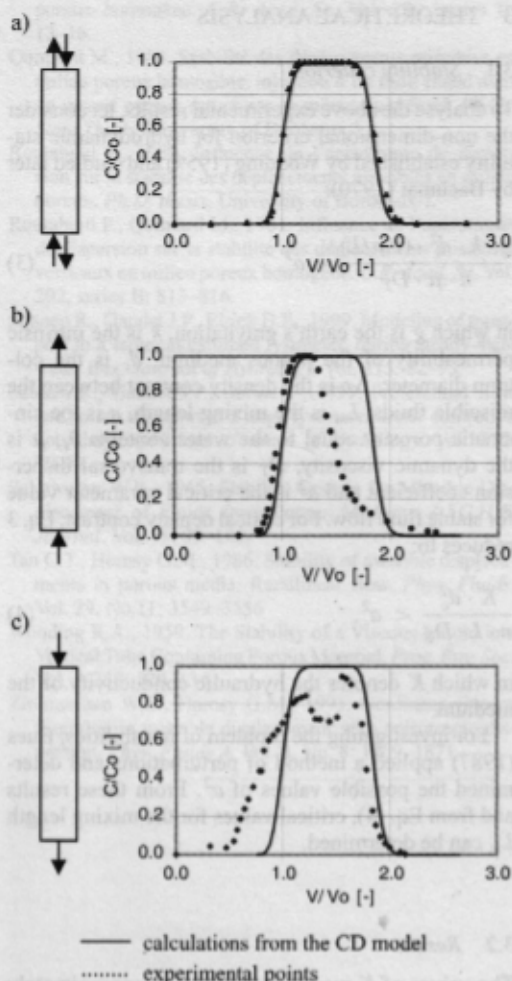


Figure 2. Experimental and calculated breakthrough curves during: a) bead size: $d_1 = 1$ mm; stable flow, b) bead size: $d_2 = 4$ mm; unstable ascending flow, c) bead size: $d_2 = 4$ mm; unstable descending flow.

gathered at the exit of the column). The retardation factor $R \approx 1.04$ denotes that there is no chemical reaction between the solutes and the porous medium. The dispersion coefficient is found to be $D_1 = 2.5 \text{ cm}^2/\text{h}$.

When the bead size is $d_2 = 4$ mm (cases b and c), the flow direction has an influence (Fig. 2b, 2c). Both curves are significantly different: on Fig. 2b a tailing effect appear whereas the experimental curve 2c is oscillating. In both cases, the mass balance is low ($MB_2 = 0.75$) and the experimental curves are non-symmetrical. The dispersion coefficient determined from the rising part of curve 2b is found to be $D_2 = 4 \text{ cm}^2/\text{h}$.

3 THEORETICAL ANALYSIS

3.1 Stability criterion

To analyse the above experimental results, let consider the non-dimensional criterion for hydrodynamic stability established by Wooding (1959) and studied later by Bachmat (1970):

$$\frac{g \cdot k \cdot d_c^2 \cdot (\Delta\rho/L)}{n \cdot \mu \cdot D_T} < a^2, \quad (3)$$

in which g is the earth's gravitation, k is the intrinsic permeability of the porous medium, d_c is the column diameter, $\Delta\rho$ is the density contrast between the miscible fluids, L_m is the mixing length, n is the cinematic porosity equal to the water contents θ_s , μ is the dynamic viscosity, D_T is the transversal dispersion coefficient and a^2 is the critical parameter value for stable fluid flow. For critical density contrast, Eq. 3 reduces to:

$$\frac{K \cdot d_c^2}{n \cdot L \cdot D_T} < a^2, \quad (4)$$

in which K denotes the hydraulic conductivity of the medium.

For investigating the problem of instabilities, Bues (1987) applied a method of perturbations and determined the possible values of a^2 . From these results and from Eq. (4), critical values for the mixing length L_m can be determined.

3.2 Results

The values of K were estimated to be approximately 10 cm/h and 40 cm/h for the glass beads of diameter 1 mm and 4 mm, respectively. When the bead size is of 4 mm, we obtained a critical value for the mixing length of $L_{min} = 35.23$ cm. The critical length L_{min} is therefore greater than the length of the column L , which means that the stability conditions cannot be met. This is in agreement with the experimental results. For beads of diameter 1 mm, L_{min} is found to be 1.85 cm: the stability conditions can therefore be reached.

4 DISCUSSION OF RESULTS

In order to explain the occurrence of instabilities, we examine the stabilizing and destabilizing mechanisms. The stabilizing mechanisms are: viscosity, dispersion and increase of fluid velocity, while the destabilizing mechanisms include gravitation, decrease of fluid velocity and increase of pore size (related to the bead size).

4.1 Stable fluid flow (Figure 2a)

When the most concentrated solute B pushes the less concentrated solute A, the destabilizing force which is acting is gravity. In this case, the pore size is small, and the viscosity forces and dispersion effects are sufficiently large to balance the destabilizing effect of gravity. As a consequence, instabilities which may occur in the mixing zone between both miscible fluids are naturally reduced. Even if some local instabilities appear over the interface, the global flow remains stable whatever the flow direction and the configurations of solutes (the most concentrated solute above the less concentrated solute or inversely).

4.2 Unstable upward fluid flow (Figure 2b)

In this case, the most dense solute B is injected into the column and pushes up the less dense solute A. In this configuration, the fluid flow is stable (the rising part of the breakthrough curve of Figure 2b fits well the theoretical curve calculated with the CD model) despite large size of glass beads. When the injection of solute B is stopped, solute A is then injected. Solute B is thus pushed by the less dense solute A. The viscosity forces and dispersion effects are insufficient to balance the gravity force. Instabilities appear which can be seen by the occurrence of small fingers and by the tailing effect on the descending part of the breakthrough curve on Figure 2b. Fingering occurs as a result of solute configuration: the most concentrated solute is located above the less concentrated solute.

4.3 Unstable downward fluid flow (Figure 2c)

In this case, instabilities occur on the rising part of the breakthrough curve (the densest solute is located above the less dense solute). However, the flow remained stable on the descending part of the curve when solute A pushes down solute B.

5 CONCLUSIONS

On the basis of the above experimental and theoretical results, we conclude that instabilities may occur when the most concentrated solute is located above the less concentrated solute and when the pore size is quite large.

In order to accurately interpret non-uniformities on breakthrough curves, a rectangular impulse should be injected during both ascending and descending flow: obtaining identical curves for both flow directions ensures the absence of instabilities.

REFERENCES

- Bachmat Y., Elrick D.E., 1970. Hydrodynamic Instability of Miscible Fluids in a Vertical Porous Column. *Water Resour. Res.* Vol. 6, No. 1: 156-171.

Bues M.A., Triboix A., Zilliox L., 1987. Stabilité des déplacements miscibles verticaux dans un milieu poreux en régime de dispersion mécanique. *Journal of theoretical and applied mechanics*. Vol. 6, No. 5: 727-758.

Dumore J.M., 1964. Stability consideration in downward miscible displacement. *Soc. Petrol. Engrs Journal*. XII: 356.

Hill S., 1952. Channelling in packed columns. *Chem. Eng. Sci.* 1, 247.

Heller J.P., 1965. Onset of Unstability Patterns Between Miscible Fluid in Porous Media. *Journal of Applied Physics*. Vol. 37: 1566-1579.

Homsy G.M., 1987. Viscous Fingering in Porous Media. *Ann. Rev. Fluid Mech.* 19: 271-311.

Jury W.A., Roth K., 1990. Transfer Functions and Solute Movement through Soil. Theory and Application. Birkhäuser Verlag, Basel.

Manickam O., Homsy G.M., 1995. Fingering instabilities in vertical miscible displacement flows in porous media. *J. Fluid Mech.* Vol. 288: 75-102

Pallud C., 2000. Etude multi-échelles du fonctionnement hydrodynamique et microbiologique d'un sol soumis à un apport de soluté: application à l'ammonium et au 2,4-D. *Ph.D. thesis*, University of Joseph Fourier, Grenoble.

Perrine R.L., 1961. The Development of Stability Theory for Miscible Liquid-Liquid Displacement. *S.P.E. Journal*, III: 17-25.

Quitard M., 1979. Stabilité des déplacements miscibles verticaux en milieu poreux. *Ph.D. thesis*, University of Bordeaux-I.

Quitard M., Combarnous M., 1980. Stabilité des déplacements miscibles non isothermes verticaux en milieu

poreux homogène. *C.R. Acad. Sc.* Vol. 290, series B: 13-16.

Quitard M., 1983. Stabilité des déplacements miscibles en milieu poreux homogène: injection d'un fluide chaud dans un massif poreux saturé par ce même fluide froid. *Ph.D.-State Thesis*, University of Bordeaux-I.

Routaboul F., 1980. Influence de l'anisotropie de dispersion sur la stabilité des déplacements miscibles en milieu poreux. *Ph.D. thesis*, University of Bordeaux-I.

Routaboul F., Quintard M., 1981. Influence de l'anisotropie de dispersion sur la stabilité des déplacements miscibles verticaux en milieu poreux homogène. *C.R. Acad. Sc.* Vol. 292, series B: 813-816.

Schoen R., Gaudet J.P., Elrick D.E., 1999. Modeling of transport in a large undisturbed lysimeter, during steady-state water flux. *Journal of Hydrology*. Vol. 215: 82-93.

Schoen R., Gaudet J.P., Bariac T., 1999. Preferential flow and solute transport in a large lysimeter under controlled boundary conditions. *Journal of Hydrology*. Vol. 215: 70-81.

Schowalter W.R., 1965. Stability Criteria for Miscible Displacement of Fluids from Porous Medium. *A.I.C.H.E. Journal*. Vol. 11: 99-105.

Tan C.T., Homsy G.M., 1986. Stability of miscible displacements in porous media: Rectilinear flow. *Phys. Fluids*. Vol. 29, No.11: 3549-3556

Wooding R.A., 1959. The Stability of a Viscous Liquid in a Vertical Tube Containing Porous Material. *Proc. Roy. Soc.* Vol. A 252: 120-134.

Zimmerman W.B., Homsy G.M., 1991. Nonlinear viscous fingering in miscible displacement with anisotropic dispersion. *Phys. Fluids A*. Vol. 3, No. 8: 1859-1871.

where various experimental data obtained for this type of flow show that the macroscopic flow equations have the form:

$$\text{grad} P = -\frac{\mu}{K} \nabla \phi + \beta \rho \nabla \phi \quad (1)$$

where P and ϕ are the macroscopic pressure and the macroscopic flow velocity, μ is the viscosity, K is the apparent permeability, the empirical correction to the Darcy law, function β is a dimensionless form of flow velocity. The term "apparent" is used to emphasize that this value may differ from the real medium permeability.

For a flow which is 1D at the macroscale, this equation may be written in the scalar form:

$$-\frac{\partial P}{\partial x} = \frac{\mu}{K} v + \beta \rho v^2 \quad (2)$$

where ρ is the density, β is the empirical " inertia coefficient".

According to the classical theory, the non-linear term is treated as the marginal result of all the nonlinear effects of inertia phenomena caused by irregularities of flow channels. Among the various forms of this macroscopic there are two very important phenomena: the first is the pore inertia effect which consists of

the work of this classical theory the marginal pore inertia effect in porous medium must be zero. This is a version of the known D'Alembert paradox. To explain the true origin of the non-linear term observed experimentally, a series of numerical experiments has been performed, these have prompted a new theoretical explanation for the non-linear correction to Darcy's law.

2. FLOW AND MEDIUM MODELS

Let us examine the single-phase, steady-state incompressible flow in porous medium of periodic structure with a period L . Let the period be small compared to the macroscopic size of the domain. Let the medium be isotropic at the macroscale. Let a single period of the medium occupy the domain $\Omega = \Omega_1 \cup \Omega_2 \cup \Omega_3$, $\Omega_1 = \Omega_2 = \Omega_3$, where Ω_1 is the porous space, Ω_2 is the solid body. The boundary $\partial\Omega_1$ of sub-domain Ω_1 consists of two non-intersecting parts: $\partial\Omega_1 = \partial\Omega_1^* \cup \Gamma$, where $\partial\Omega_1^*$ is the interface between the solid and the porous space, and $\Gamma = \Gamma_1 \cup \Gamma_2 \cup \Gamma_3$ is that part of the external boundary of the unit period Ω , which crosses sub-domain Ω_1 .

Shown in Fig. 1 are the two types of media that have been considered.